

Observer-Based Monitors for Electromechanical Dynamics in Power Networks¹

E. Scholtz
ABB Inc. USCRC
Raleigh, NC, USA
ernst.scholtz@us.abb.com

G. C. Verghese
MIT
Cambridge, MA, USA
verghese@mit.edu

B. C. Lesieutre
LBNL
Berkeley, CA, USA
BCLesieutre@lbl.gov

Abstract - In this paper we demonstrate how dynamic observers can be used to monitor system-wide electromechanical (or “swing”) dynamics in power systems. We illustrate how to design these observer-based monitors, which can dynamically estimate the state of the system or detect and identify specific occurrences of faults in the system, in the presence of disturbances and uncertainty. We demonstrate our monitor design approach on a small 3-bus and an intermediate-sized 179-bus power system model.

Keywords - System-Wide Monitoring, Observers, State Estimation, Fault Detection and Isolation

1 Introduction

In this paper we discuss two types of monitoring tasks: dynamic state estimation, and fault detection and isolation (FDI). Power system state estimation in the traditional sense has mainly focused on *static* estimation from *redundant* measurements [1]. There also exists literature in the power system field on dynamic-state estimation, which deals with: *recursive* processing of measurements, but with *no dynamics* in the state [2, 3]; or *slow-speed* state dynamics induced by *load* variations, and these dynamics are estimated on-line in various ways using load forecasting ideas [2, 4].

Swing-state estimation implies estimating the dynamic variations of bus angles and generator speeds, but not the bus-voltage magnitudes. The ideas and approaches set forth in this paper can be extended to include voltage dynamics of the system, but such an extension is left for future explorations. Literature discussing dynamic swing-state estimation can be found in [5, 6, 7, 8, 9, 10]. Modir et al. [5] used a linear Kalman filter to estimate the small-signal swing state of a power system. The filter was used in a modular setup, where the steady-state voltage magnitudes and bus angles were updated by a static state estimation scheme. In [6], the single-machine, infinite-bus case was investigated and a nonlinear gain-scheduled observer was used to estimate the swing state of the single machine (voltage magnitudes were assumed constant). In [7], a recurrent artificial neural network was used to estimate the swing state of a network while assuming that voltages are constant. In [9, 10], a mixture of generator and load buses was modeled via a nonlinear Differential Algebraic Equation (DAE) swing model, in contrast to the linear collapsed all-generator network investigated in

[8]. In [8, 9], Linear-Quadratic-Estimator gains were designed using a linearized *state-space* model. Such a gain was then used in a nonlinear-DAE extension of the linear state-space observer.

In this paper we highlight our extensions from [9] as detailed in the thesis [10]. We demonstrate how to design observer-based monitors, using a novel graphical design approach developed in [10]. The observer can function in the presence of unknown system changes (e.g. load changes, generation changes, line outages) that were not explicitly studied in [5, 6, 8], in order to achieve different functions (i.e., state estimation or FDI). (Only state estimation was investigated in [5, 6, 7, 8, 9].) This intuitive design approach makes it potentially feasible to realize observers for potentially large systems without running into intractable computation issues.

In [11], model-free methods (i.e., signal processing approaches) using local measurements are employed to estimate and predict power-system swings and their damping. In order to compute good estimates the investigated methods rely on persistently excited signals with high signal-to-noise ratios. The author concludes that real-time monitoring of electromechanical oscillation frequency and damping is possible for systems with a single dominant mode, but also determines that one- and M -step-ahead predictors' performances were not satisfactory. The observer-based monitoring framework discussed in this paper has the potential to be used for constructing state predictors. The model used in the observer provides the monitor with the ability to predict future system behavior, when the observer simulator runs faster than real-time. The observer runs open loop during the prediction stage and relies on the internal model to predict system behavior. When measurement updates are available, the estimation loop is closed, bringing the estimate closer to the system state.

A hybrid simulation technique that joins the simulation and measurement worlds of power system planning and operation was introduced in [12]. This tool simulates the dynamics of a reduced part of a network. High-quality synchronized measurements are used as external driving variables to this system, aggregating the influences of the rest of the network on the reduced part. Our observer-based framework can also be used to create an on-line monitor for such a reduced network. Both our approach and the one in [12] assume that a dynamical model of the

¹This work was supported under the AFOSR DoD URI F49620-01-1-0365: “Architectures for Secure and Robust Distributed Infrastructures”.

reduced network is available. The boundary of the reduced network in [12] is drawn at the buses where the measurements are taken, whereas with our approach we have some flexibility in drawing this boundary (i.e., we can expand or contract it around the locations of the ‘boundary’ measurements) and our approach also permits advantage to be taken of additional measurements inside the boundary in constructing an observer. In effect, [12] constructs an open-loop reduced-order observer (i.e., an uncorrected simulator of a part of the network), whereas our approach permits the use of a correction term based on measurements internal to the reduced network.

The rest of the paper is organized as follows. In Section 2, we discuss the swing model of a power system briefly. Section 3 discusses the observer structure. In Section 4, we introduce the novel observer design method. In Section 5, we illustrate the working of our observer-based monitors. In Section 6, we summarize our results and discuss additional design issues.

2 Electromechanical Model of Power Systems

We focus on the swing model associated with transmission-level power system models, and assume that loads do not exhibit dynamics on the time-scale of interest. These loads can represent aggregated load areas or distribution networks. In this paper we view these loads as constant powers that can change in an abrupt fashion (e.g., load shedding). We furthermore assume that voltage-bus magnitudes are controlled at 1p.u., effectively omitting voltage dynamics. The nonlinear DAE swing model has the following functional form:

$$M\dot{x} = f(x, u, w), \quad (1)$$

where: $x = [\theta'_g \ \omega \ \theta'_l]^\top \in \mathbb{R}^n$ is the vector of internal variables of the above DAE; θ'_g is a vector of machine angles at generator buses; θ'_l is a vector of voltage angles at load buses; ω is a vector of generator speed deviations from synchronous; M is singular because of the lack of dynamics at load buses; n is equal to the number of buses plus the number of generator buses in the network. The elements of θ'_g and ω are state variables, while the elements of θ'_l are algebraic variables. The elements of f are nonlinear functions (obtained from the power flow equations on the network and the swing equations of the generators) of x , the known inputs u and the unknown inputs w . u is obtained from solving the dispatch problem and some sources of w are discussed in Section 3.

The measurements taken in the system are denoted by $y = g(x) + v$, where g is a nonlinear function x and v is the vector of measurement disturbances. In [10], we considered five types of measurements: bus angles; generator speeds; power injected into the network at the buses; power flow on the lines; and angle differences across lines. In this paper we confine our attention to bus angle measurements.

3 Observer-Based Monitors

In order to monitor the dynamical system (1), we advocate the use of an observer. We can use the same observer framework to create two types of monitors: a state-estimation monitor and a FDI monitor. We will discuss these two types of monitors shortly.

We use a nonlinear dynamic model of the system in the observer, to accumulate over time and interpolate over space (i.e., over the entire network) the information contained in measurements obtained from a select set of sensors. The proposed observer has the form

$$M\dot{\hat{x}} = f(\hat{x}, u, w = 0) + Lz \quad (2)$$

$$z = y - \hat{y}, \quad (3)$$

where M , f , u , w are as defined in (1), \hat{x} is the internal variables of the DAE observer, L is the observer gain, and $\hat{y} = g(\hat{x})$. The designed observer will have the same number of internal variables \hat{x} as x in the model (1). The number of design variables in L is equal to $n \times q$, where q is the number of measurements y .

Other possible nonlinear observers were considered in [10], but (2) was selected because existing nonlinear time-domain simulators of power systems can be used to partially realize (2). In order to fully realize (2) we provide real-time inputs that are proportional to $z = y - \hat{y}$.

In [10] we settled on using linear techniques to design L , hence we will focus on the following linearized version of (1) and y ,

$$M\dot{\tilde{x}} = A\tilde{x} + B\tilde{u} + Ew \quad (4)$$

$$\tilde{y} = C\tilde{x} + v, \quad (5)$$

where a vector in the nonlinear system can be expressed as $\zeta = \bar{\zeta} + \tilde{\zeta}$ with $\bar{\zeta}$ being the steady-state vector and $\tilde{\zeta}$ the vector of deviations from this steady-state (assumed small when deriving the linearized model). For this linearized model we have $A \triangleq \left[\frac{\partial f}{\partial x} \right]_{\bar{x}, \bar{u}, \bar{w}}$, $B \triangleq \left[\frac{\partial f}{\partial u} \right]_{\bar{x}, \bar{u}, \bar{w}}$, $C \triangleq \left[\frac{\partial g}{\partial x} \right]_{\bar{x}, \bar{u}, \bar{w}}$, $E \triangleq \left[\frac{\partial f}{\partial w} \right]_{\bar{x}, \bar{u}, \bar{w}}$, $\bar{w} = 0$ and $\bar{v} = 0$.

Linearizing (2) at the current operating point we obtain the linearized observer

$$M\dot{\hat{\tilde{x}}} = A\hat{\tilde{x}} + B\tilde{u} + L(\tilde{y} - \hat{\tilde{y}}) \quad (6)$$

$$\hat{\tilde{y}} = C\hat{\tilde{x}}, \quad (7)$$

where M, A, B, C are as defined earlier. We stress that we only consider (6) and (7) for design of L and not for observer realization. Defining $e = \tilde{x} - \hat{\tilde{x}}$ a DAE system for the observer-based monitoring problem is found as

$$M\dot{e} = (A - LC)e + Ew - Lv \quad (8)$$

$$r = QCe, \quad (9)$$

where r is defined as the residuals and we use $(M, A - LC, E, QC)$ as shorthand for this DAE-monitor system.

The DAE swing model (4) and (5) can be expressed as an equivalent state-space system, for which we can design a linear state-space observer that generally has smaller dimension than (6). We followed this approach in [9], but in [10] we showed that if we keep the system in DAE form and design a DAE observer we have additional degrees of freedom for observer design of systems where unknown inputs w are present.

Sources of Unknown Signals w

Various perturbations and uncertainties in the power system can be modelled in the form Ew . Perturbations such as load/generation changes, generator outages, line flow perturbations (e.g., line outages or short circuits) as well as uncertainties of line parameters and generator inertias.

An unknown line change occurring on line h will impact the entries in A associated with the contributions of line h . In [10], we show that each line change (or uncertain line parameter) will have an associated rank one perturbation matrix \tilde{A}_h in (4), for which we can model $\tilde{A}_h \tilde{x} = Ew$.

Another source of w can be changes in adjacent unmodelled power systems. In this case our study area is given by (4) and the influences from the rest of the network on our study area can be thought of as w signals. We can thus make our estimator insensitive to changes in adjacent networks, or make it sensitive to indicate that a neighbor is experiencing problems.

Before discussing our observer design method we highlight the types of monitors studied in this paper.

State-Estimation Monitor

The purpose of the state-estimation monitor is to have \hat{x} be an estimate of x , forcing e to tend to zero in the presence of nonzero unknown signals w and for nonzero initial conditions $e(0) = x(0) - \hat{x}(0)$. In this paper we assume that $e(0) = 0$ and we are interested in forcing as many entries in $G_{ew}(s) = (sM - A + LC)^{-1}E$ to zero as s tends to zero. Here $G_{ew}(s)$ is the transfer function matrix from unknown signals w to errors e . In order to achieve this requirement we have L available for design. Observer design in the presence of unknown signals is challenging, but the design method we introduce in the next section provides an intuitive approach to accomplish this task.

FDI Monitor

We partition w to distinguish between faults we want to identify α and disturbances we want to attenuate β , and accordingly form E_α and E_β from E . The objectives of the FDI monitor are to have $G_{r\alpha}(s) = QC(sM - A + LC)^{-1}E_\alpha$ be upper triangular — to aid with fault isolation and identification — and have $G_{r\beta}(s) = QC(sM - A + LC)^{-1}E_\beta$ be identical to zero

for all s [13]. This will insure that the filter's residuals r will be significantly nonzero when α is nonzero, and r will not be impacted by nonzero β 's. In [13], the authors provide necessary and sufficient conditions the system $(M = I, A, E, C)$ has to satisfy in order for the FDI problem to be generically solvable.

Number and Placement of Measurements

In [13], the generic solvability of the FDI problem is investigated for structured state-space systems of the form (4) and (5) with $M = I$ and $v = 0$. The authors provide necessary and sufficient conditions under which the FDI problem for a system $(M = I, A, E, C)$ has a solution. The authors do not discuss the design of Q and L , but their result is useful when measurements are selected/placed for observer-based monitor design.

4 Graphical Observer Design

In [13, 14], generic properties of linear structured systems (such as controllability) are studied in a qualitative way. In these studies directed graphs are associated with linear structured systems. The structure in such a system is obtained from all the zero entries in the system matrices, and all the nonzero entries are viewed as free parameters. Our interest is in the use of graphical techniques to display system structure, but results on generic properties are of less interest, since our models don't typically have free parameters in the sense of [13, 14].

For the linear structured system $(M, A - LC, E, QC)$ given by Equations (8) and (9) (with $v = 0$) we have $e \in \mathbb{R}^n$; $w \in \mathbb{R}^m$; and $r \in \mathbb{R}^p$. We can associate a directed graph $\mathbf{G}(\mathbf{V}, \mathbf{Z})$ with this system. \mathbf{V} denotes the set of vertices of the directed graph and is obtained by forming $\mathbf{V} = \mathbf{E} \cup \mathbf{W} \cup \mathbf{R}$, where $\mathbf{E}, \mathbf{W}, \mathbf{R}$ are the sets $\{e_1, e_2, \dots, e_n\}$, $\{w_1, w_2, \dots, w_m\}$, $\{r_1, r_2, \dots, r_p\}$ respectively. Hence the variables of the system description form the vertices of the directed graph.

The arc set \mathbf{Z} is obtained by forming the union of $\mathcal{E}_w = \{(w_i, e_j) | E_{ji} \neq 0\}$, $\mathcal{E}_e = \{(e_i, e_j) | A_{ji} \neq 0\}$, $\mathcal{E}_m = \{(e_i, e_j) | M_{ji} \neq 0\}$, $\mathcal{E}_r = \{(e_i, r_j) | Q_{j,:} C_{:,i} \neq 0\}$, and $\mathcal{E}_l = \{(e_i, e_j) | L_{j,:} C_{:,i} \neq 0\}$ (where $Q_{j,:}$ and $L_{j,:}$ represents rows j of Q and L respectively, and $C_{:,i}$ represents column i of C). The above edge weights are obtained from the system matrices, except for \mathcal{E}_l , which we will design. In the studies discussed in [13, 14], the authors view the edge weights of the arcs as free parameters and are not concerned with the quantitative information contained in these weights. We will use these weights, which are a function of the current operating point, for observer design.

Due to the diagonal structure of M the set \mathcal{E}_m will consist of self-cycles at the differential variable vertices [14]. These additional loops do not provide us with extra insight into observer design and they will not be drawn in

the directed graph example that will follow. Also, whenever $QC = I$ we will not explicitly draw the \mathcal{E}_r edges.

We will demonstrate our novel observer-design approach on a three-bus power system example, which consists of one generator and two loads as shown in Figure 1. This system has three bus angles, one generator speed and $M = \text{diag}([1 \ 1 \ 0 \ 0])$.

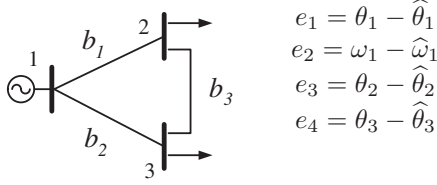


Figure 1: Three-bus system and the definition of the elements e_i in E .

We assume that the system is subject to an unknown load change at bus 3, i.e., $E = [0 \ 0 \ 0 \ 1]'$, and that we measure the voltage angle at bus 2, i.e., $C = [0 \ 0 \ 1 \ 0]$. The system matrix A is given as

$$A = \begin{bmatrix} 0 & 1 & 0 & 0 \\ -b_1 - b_2 & -d & b_1 & b_2 \\ b_1 & 0 & -b_1 - b_3 & b_3 \\ b_2 & 0 & b_3 & -b_2 - b_3 \end{bmatrix}.$$

The unassigned observer gain is given as $L = [l_1 \ l_2 \ l_3 \ l_4]'$, and we can now write

$$A - LC = \left[\begin{array}{ccc|cc} 0 & 1 & -l_1 & 0 & 0 \\ -b_1 - b_2 & -d & b_1 - l_2 & b_2 & \\ b_1 & 0 & -b_1 - b_3 - l_3 & b_3 & \\ b_2 & 0 & b_3 - l_4 & -b_2 - b_3 & \end{array} \right].$$

We will only highlight our design approach and the interested reader is referred to [10] for more details:

1. Draw $\mathbf{G}(\mathbf{V}, \mathbf{Z})$ for the error dynamical system $(M, A - LC, E, I)$. See Figure 2(a) for the design setup.
2. Eliminate forward paths (by choosing the values of L appropriately) in $\mathbf{G}(\mathbf{V}, \mathbf{Z})$ from the e -vertex where the \mathcal{E}_l arcs originate (i.e., the measured variable), **except** the forward path to the e -vertex directly impacted by w . (This latter edge has a weight of $\xi = b_3 - l_4$.) For our example we choose $l_1 = 0$, $l_2 = b_1$, and $l_3 = -b_1 - b_3$. See Figure 2(b) for the design result. From this figure we notice that some signal flow paths in $\mathbf{G}(\mathbf{V}, \mathbf{Z})$ were eliminated.
3. ξ can now be chosen in order to realize the two types of monitors for:
 - state estimation by choosing ξ to be large in order to attenuate the effect of **disturbance** w . $G_{ew}(s) = [0 \ 0 \ \frac{1}{\xi} \ 0]'$.

- FDI by choosing ξ small in order to amplify the effect of **fault** w . $G_{rw}(s) = \frac{1}{\xi}$.

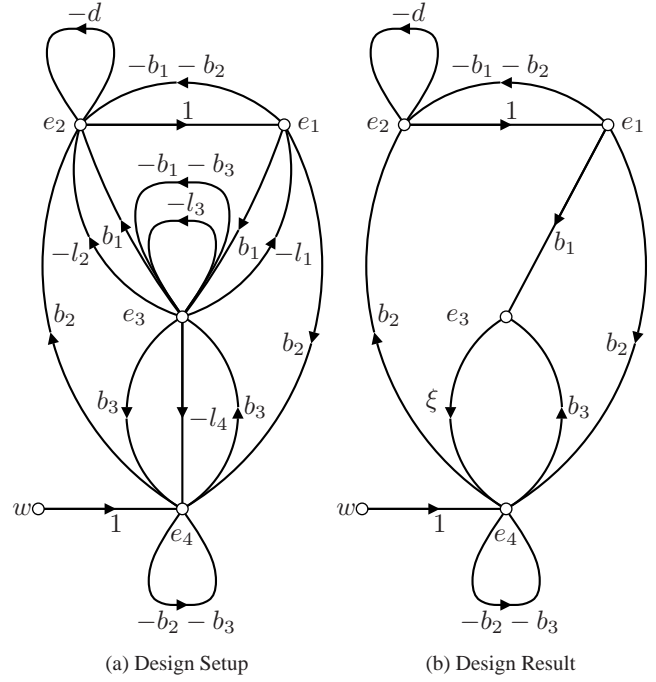


Figure 2: Graphical Observer Design with $C = [0 \ 0 \ 1 \ 0]$.

5 Monitor Examples for an 179-Bus System

In this section we study an 179-bus aggregated version of the Western States Coordinating Council (WSCC) power system². The one-line diagram of this system is shown in Figure 3³. The system consists of 29 generators and 150 load buses and the model of form (1) for this system has 208 internal variables with 58 state variables and 150 algebraic variables. In Figure 3 we indicate the locations of angle measurements we will use for observer design: $y_1 = \theta_{78}$, $y_2 = \theta_{59}$, $y_3 = \theta_{83}$, and $y_4 = \theta_2$.

In Figure 3, we also indicate the locations where unknown power injections/extractions w_1 to w_4 can occur. In our example we assume that occurrences of these unknown inputs are in the form of pulses. In Table 1 the various pulses are described.

In this section we will illustrate the functioning of the two types of monitors we discussed in Section 3.

In all of the following simulations we assume that the generators are uncontrolled. We introduce some parametric model uncertainty into the system model, by assuming that the parameters of the system are randomly perturbed by 10% (using an uniform distribution) around their nominal values. We use these nominal values in the realization of the observer. In this paper we do not design the

²We would like to thank Professor A. G. Phadke at VPI&SU, Professor V. Vittal at Arizona State University and Xiaoming Wang at Iowa State University for sharing the aggregated WSCC 179 bus model with us.

³A special thank you to Xiaoming Wang for providing us with this one-line diagram.

observer to be robust to these introduced parameter uncertainties, because we want to demonstrate how well the observer performs even in the presence of moderate parametric model uncertainty.

	$w_1 = \tilde{P}_{67}$	$w_2 = \tilde{P}_{41}$	$w_3 = \tilde{P}_{100}$	$w_4 = \tilde{P}_{85}$
[p.u.]	-1	1	1.5	-1.5
t_d [s]	[1, 3]	[2.5, 5]	[0.001, 7]	[0.001, 7]

Table 1: Amplitude and duration of perturbations and faults.

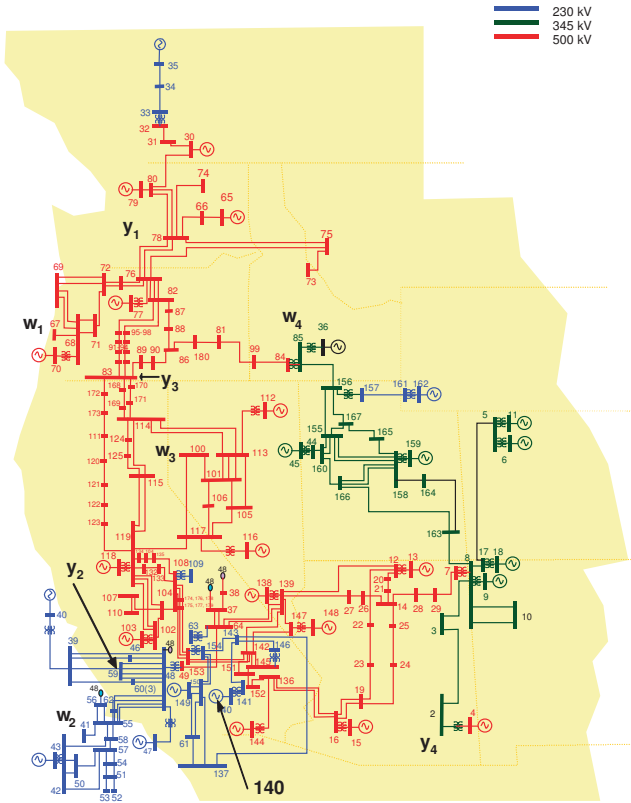


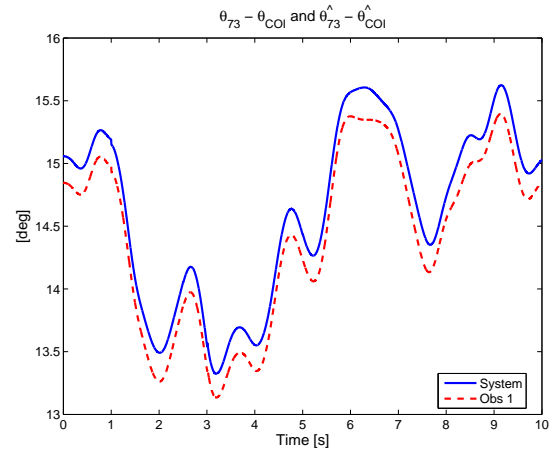
Figure 3: One-line diagram of an aggregated WSCC network, illustrating fault, disturbance and measurement locations. (Acknowledgement: A. G. Phadke, V. Vittal, X. Wang.)

We also assume that the initial conditions of the system and the observer are the same in order to avoid solving the power flow problem for the perturbed system before commencing the dynamic simulation. This approach also limits the impact of transients due to a large mismatch in initial conditions of the system $x(0)$ and the observer $\hat{x}(0)$. In this paper we do not design our observer to attenuate the effect of such a mismatch $e(0)$, and hence we choose $x(0) = \hat{x}(0)$ in order to limit the impact of a nonzero $e(0)$ on the performance assessment of the observer. In practice we can limit the effect of nonzero $e(0)$ on the desired monitoring task by using additional measurements to move the eigenvalues of the $(M, A - LC)$ system in order to force transient trajectories of e that are driven by $e(0)$ to decay to zero.

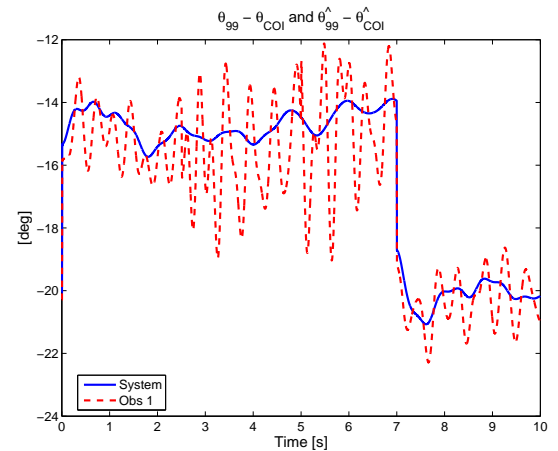
State Estimation

As part of the observer design we associate each measurement with an unknown signal w . In this example we as-

sociate y_i with w_i for $i \in [1, \dots, 4]$. In this example all w_i 's given in Table 1 are seen as disturbances, and each ξ_i (as defined in Section 4) is set large (i.e., 1×10^4). We also found that by choosing the ξ_i 's to be 1×10^4 we had $\|A\|_2 = \|A - LC\|_2$. The other nonzero entries in L are obtained from extracting entries from A as discussed in Section 4. After constructing L we check whether $(M, A - LC)$ is stable, and if this is indeed the case we use L in the realization of (2).



(a) $\theta_{73} - \theta_{coi}$ vs. $\hat{\theta}_{73} - \hat{\theta}_{coi}$



(b) $\theta_{99} - \theta_{coi}$ vs. $\hat{\theta}_{99} - \hat{\theta}_{coi}$

Figure 4: Selected x trajectories of the system (solid lines) compared to their corresponding \hat{x} trajectories.

In the sub-figures of Figure 4, two system trajectories are compared to their corresponding observer estimates, in response to the events described in Table 1. In these figures system angles θ_i 's are expressed relative to the evolution of the center-of-inertia angle θ_{coi} . The observer angles $\hat{\theta}_i$'s are expressed relative to the observer's $\hat{\theta}_{coi}$. The two angle trajectory comparisons shown in Figures 4(a) and 4(b) were identified by evaluating $\|\theta_i - \hat{\theta}_i\|_2$ for each of the 179 bus angles and then choosing the one with the minimum norm (Figure 4(a)) and the one with the maximum

norm (Figure 4(b)). From both of these plots we notice that the observer's estimates track the trend of the system trajectories satisfactorily, even though the estimate in Figure 4(b) has higher frequency dynamics superimposed.

Fault Detection and Isolation

For this example y_1 and y_2 are used to detect the occurrences of w_1 and w_2 respectively. We use y_3 and y_4 to attenuate the effect of nonzero w_3 and w_4 disturbances. From Section 4 we know that if w_k is a fault we want to detect, we set ξ_k to be very small, and if w_k is a disturbance, ξ_k is set very large. For our current example we set $\xi_1 = 50$, $\xi_2 = 50$, $\xi_3 = 1 \times 10^4$, and $\xi_4 = 1 \times 10^4$. After constructing L we check whether $(M, A - LC)$ is stable, and if so we use L in the realization of (2).

In Figure 5, the response of the designed observer-based monitor is shown in response to the events described in Table 1. We note that the monitor attenuates the occurrence of disturbances w_3 and w_4 , as well as *detects* and *isolates* the occurrences of w_1 and w_2 that occur separately as well as simultaneously. We notice that z_3 and z_4 , which are driven by the disturbances, stay approximately zero and can be left out of the FDI monitor by choosing $Q = \begin{bmatrix} I_2 & 0 \end{bmatrix}$.

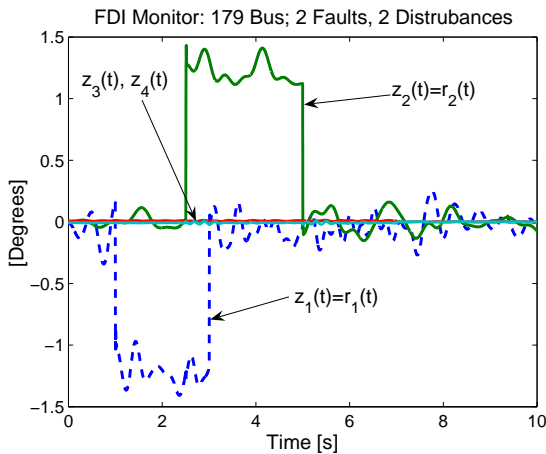
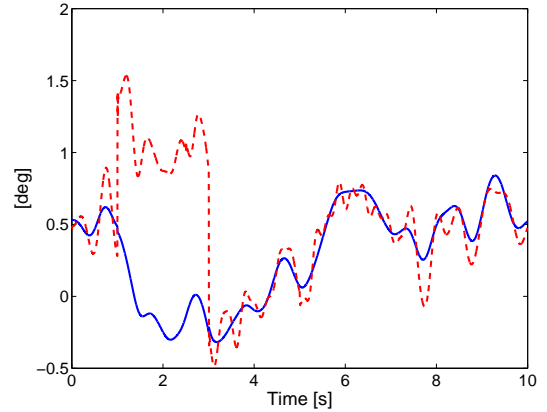
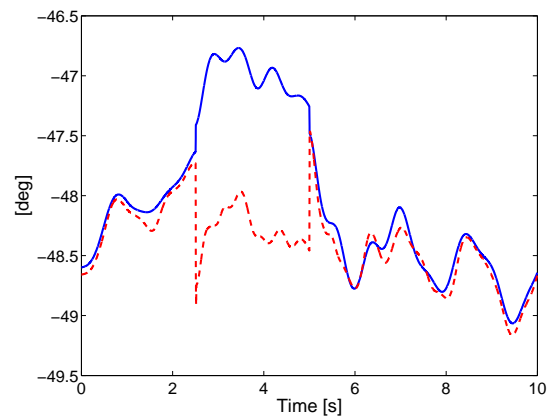


Figure 5: Output of observer-based monitor in response to the events described in Table 1. Here $z = y - \hat{y}$ and $r = Qz$.

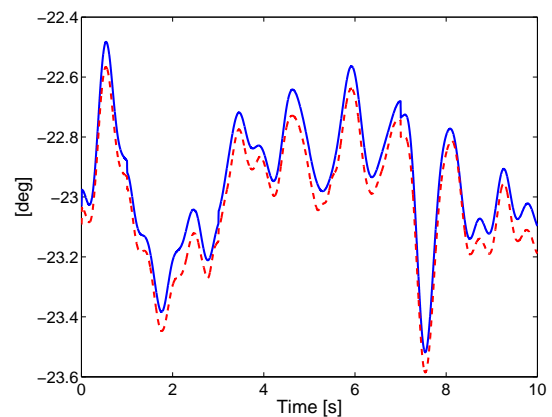
In the sub-figures of Figure 6 a select few x trajectories are compared to their corresponding \hat{x} trajectories. From Figures 6(a) and 6(b) we notice that the observer's estimates track the system trajectories, except during the event periods when faults w_1 and w_2 occur. In Figures 6(c) and 6(d) we show that the FDI monitor also provides us with a good voltage-angle estimate at bus 83 and a good speed-state estimate of the generator at bus 140. Note that the monitor does not use any speed measurements, hence the good speed estimate is due to the use of the system model in the observer realization.



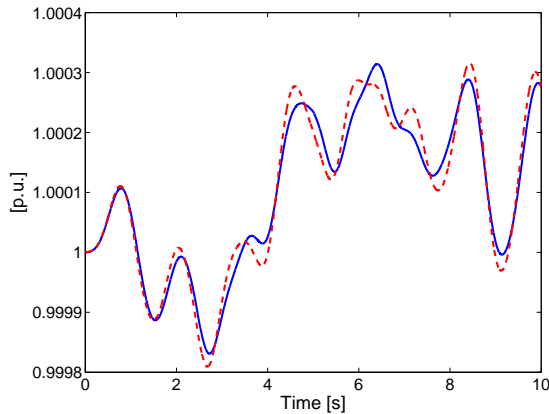
(a) $\theta_{78} - \theta_{coi}$ vs. $\hat{\theta}_{78} - \hat{\theta}_{coi}$; $y_1 = \theta_{78}$



(b) $\theta_{59} - \theta_{coi}$ vs. $\hat{\theta}_{59} - \hat{\theta}_{coi}$; $y_2 = \theta_{59}$



(c) $\theta_{83} - \theta_{coi}$ vs. $\hat{\theta}_{83} - \hat{\theta}_{coi}$; $y_3 = \theta_{83}$



(d) ω_{140} vs. $\hat{\omega}_{140}$

Figure 6: Selected x trajectories of the system (solid lines) compared to their corresponding \hat{x} trajectories.

6 Conclusions

In this paper we demonstrated how observer-based monitors can readily be designed for an 179-bus power system model by using a novel graphical observer-design technique developed in [10]. We discussed the design of two types of observer-based monitors, i.e., the state-estimation monitor and the fault-detection-and-isolation monitor. We demonstrated the design and performance of a fault-detection-and-isolation monitor on an 179-bus power system model.

This graphical observer-design technique is powerful in designing the steady-state output of the monitor, but it provides no stability guarantees for the monitoring system. After designing the desired steady state output, little to no degrees of freedom are left to move the eigenvalues of $(M, A - LC)$. If the filter is unstable, extra measurements can be added in order to move the eigenvalues of the $(M, A - LC)$ system. For such situations we propose a dual design approach, where we first identify the unknown inputs, then use specific measurements to achieve the desired monitor task. In the second step we use additional measurements for the sole purpose of moving the eigenvalues of the filter by using an eigenstructure assignment technique, to ensure that the monitor will be stable whenever the monitored system is stable.

In this paper we focussed on the swing dynamics of a power system, but the ideas presented here can be extended to include voltage dynamics. In [10] we investigated how a range of disturbances and uncertainties can be modelled, and with our design approach we can attenuate the effect of these uncertainties on the performance of our monitors.

REFERENCES

- [1] A. Monticelli, *State Estimation in Electric Power Systems*. Kluwer Academic Publishers, 1999.
- [2] P. Rousseaux, T. V. Cutsem, and T. D. Liacco, "Whither dynamic state estimation?," *Electric Power and Energy Systems*, vol. 12, no. 2, pp. 104–116, 1990.
- [3] K.-R. Shih and S.-J. Huang, "Application of a robust algorithm for dynamic state estimation of a power system," *IEEE Transactions on Power Systems*, vol. 17, pp. 141–147, February 2002.
- [4] A. Debs and R. Larson, "A dynamic estimator for tracking the state of a power system," *IEEE Transactions on Power Apparatus*, vol. 89, no. 7, pp. 1670–1688, 1970.
- [5] H. Modir and R. A. Schlueter, "A dynamic state estimator for power system dynamic security assessment," *Automatica*, vol. 20, pp. 189–200, March 1984.
- [6] J. Chang, G. Taranto, and J. Chow, "Dynamic state estimation in power system using a gain-scheduled nonlinear observer," *Proceedings of the 4th IEEE Conference on Control Applications*, pp. 221–226, 1995.
- [7] A. G. Bahbah and A. A. Girgis, "New method of generators' angles and angular velocities prediction for transient stability assessment of multimachine power systems using recurrent artificial neural network," *IEEE Transactions on Power Systems*, vol. 19, pp. 1015–1022, May 2004.
- [8] I. Stolz, "Observers and graphic displays for the swing motions of a power system," Master's thesis, Technical University of Berlin (research done at MIT), October 1994.
- [9] E. Scholtz, P. Sonthikorn, G. C. Verghese, and B. C. Lesieutre, "Observers for swing-state estimation of power systems," *North American Power Symposium*, October 2002.
- [10] E. Scholtz, *Observer-Based Monitors and Distributed Wave Controllers for Electromechanical Disturbances in Power Systems*. PhD thesis, EECS Department, Massachusetts Institute of Technology, September 2004.
- [11] M. Hemmingsson, *Power System Oscillations: Detection Estimation and Control*. PhD thesis, Lund University, 2003.
- [12] Z. Huang, R. T. Guttromson, and J. F. Hauer, "Large-scale hybrid dynamic simulation employing field measurements," *IEEE Power Engineering Society General Meeting*, 2004.
- [13] C. Commault, J.-M. Dion, O. Sename, and R. Motyeian, "Observer-based fault detection and isolation for structured systems," *IEEE Transactions on Automatic Control*, vol. 47, no. 12, pp. 2074–2079, 2002.
- [14] K. J. Reinschke and G. Wiedemann, "Digraph characterization of structural controllability for linear descriptor systems," *Linear Algebra and its Applications*, vol. 266, no. 1, pp. 199–217, 1997.